CrossMark

Enlargement of the semi-arid region in China from 1961 to 2010

Yunhe Yin[1] · Danyang Ma[1,2] · Shaohong Wu[1,2]

Abstract

Due to spatial and temporal heterogeneity in moisture conditions, the responses of arid/humid climate regions (AHCR) to climate change are complex. In this study, we delineated the AHCR of China using information about the balance of the atmospheric water supply and demand collected from 581 meteorological stations over the past 50 years. We also analyzed inter-decadal shifts and linear trends in the AHCR and examined the influence of precipitation and reference evapotranspiration. The results indicate that the semi-arid region expanded significantly over the last five decades, mainly in northwest China, northern China, and the Tibetan Plateau and, by the 2000s, had increased by 33.53% relative to its extent in the 1960s; in contrast, the arid region shrank by 20.75%. The semi-arid region grew mainly because of transfers from the arid region in western China and the sub-humid region in eastern China. The decreased reference evapotranspiration and significantly increased precipitation together contributed to the expansion of the semi-arid region in northwest China and the Tibetan Plateau over the last 50 years. In contrast, the expansion of the semi-arid region in Inner Mongolia and northern China reflects the counteractive influence of decreased reference evapotranspiration and decreased precipitation.

Keywords Arid/humid climate region · Climate change · Aridity index · Precipitation · Reference evapotranspiration

1 Introduction

The global land surface is temporally and spatially heterogeneous on a range of scales. Many studies have separated the land surface into climatic or eco-geographical regions to allow for specific investigations of regional differences and their significance for agriculture and ecosystems (Bailey 2009; Fu et al. 2001; Holdridge 1967; Huang 1989; Köppen 1931; Lin 1954; Ren and Yang 1961; Thornthwaite 1948; Zheng 1999; Zhu 1930). In recent decades, greenhouse gas and aerosol emissions have had pronounced effects on the global climate, causing an increase in the mean global surface temperature of approximately 0.85 °C (0.65–1.06 °C) between 1880 and 2012 (IPCC 2013). As the global mean temperature continues to increase, land areas are experiencing different climates at an increasingly rapid pace (Mahlstein et al. 2013). While the dynamics of moisture conditions in arid/humid climate regions (AHCR) are known to be particularly complicated, they make an important contribution to the human understanding of the impacts of climate change on, for example, desertification (Huang et al. 2016a; Reynolds et al. 2007), water resources (Crosbie et al. 2012; Scanlon et al. 2006) and crop yields (Mihailovic et al. 2015).

A range of approaches has been previously used to generate valuable information about the dynamics of climatic zones. The impacts of climate change on the spatial distribution of climatic zones on both global (Fraedrich et al. 2001; Huang et al. 2016b; Rohli et al. 2015; Rubel and Kottek 2010) and continental or regional scales (Chan et al. 2016; Engelbrecht and Engelbrecht 2016; Feng et al. 2012; Gerstengarbe and Werner 2009; Wu et al. 2010) are increasingly obvious. For example, Huang et al. (2016b) found that, based on the aridity index, semi-arid regions expanded globally by 7% from 1948–1962 to 1990–2004. Engelbrecht and Engelbrecht (2016) highlighted widespread shifts in climatic regimes using the Köppen–Geiger classification, and reported that there would be a significant expansion of

✉ Yunhe Yin
 yinyh@igsnrr.ac.cn

[1] Key Laboratory of Land Surface Pattern and Simulation, Institute of Geographic Sciences and Natural Resources Research, Chinese Academy of Sciences, 11A, Datun Road, Chaoyang District, Beijing 100101, China

[2] University of Chinese Academy of Sciences, 19A Yuquan Road, Shijingshan District, Beijing 100049, China

hot desert and steppe zones in southern Africa under future climate change.

The fact that China occupies a vast area and encompasses a wide range of climates and land surfaces, including the unique Asian monsoon climate system, means that changes in factors such as precipitation and dryness have been spatially and temporally heterogeneous. For example, studies have suggested that the climate in the semi-arid northeastern part of China has become warmer and wetter over the past 50 years, whereas it has become warmer and drier in the eastern and central regions (Yang et al. 2005). The AHCR is generally determined from the balance of the atmospheric water supply and the evaporative demand. Reference evapotranspiration (ET_o), which represents the atmospheric water demand, is critical for highlighting changes in precipitation (Dai et al. 1997), dryness (Cook et al. 2014; Dai 2011; Greve and Seneviratne 2015) and dryland dynamics (Huang et al. 2016a). As in many other regions, the ET_o has decreased significantly across extensive areas of China over the past half-century (Dolman and de Jeu 2010; Roderick and Farquhar 2002; Yin et al. 2010; Zhang et al. 2011). With spatial and temporal variations in the interactions between regional climate factors, increased knowledge of both changes in the AHCR and the causes of these changes could provide an improved understanding of regional responses to climate change. However, the combined effects of the dynamics of both the regional water supply and the evaporative demand on shifts in the AHCR over the recent past remain poorly understood, especially in the context of variations in the extent and degree of dryness, which reflect the interplay between variations in precipitation (P) and ET_o.

The major objectives of this study were therefore (1) to quantify spatial and temporal variability in the AHCR by combining the Penman–Monteith ET_o model with precipitation and (2) to investigate the influence of regional water supplies and the evaporative demand on shifts in the AHCR for the period from 1961 to 2010. The results have important implications for sustainable planning of agricultural development and eco-construction, and for protecting water resources and ecosystems.

2 Materials and methods

2.1 Materials

Quality-controlled monthly meteorological datasets of maximum and minimum air temperatures, precipitation, mean relative humidity, sunshine duration and mean wind speed from 581 meteorological stations (Fig. 1) for the period from 1961 to 2010 were used for this study. The datasets were provided by the Climatic Data Center (CDC) of the National Meteorological Information Center (NMIC) of the Chinese
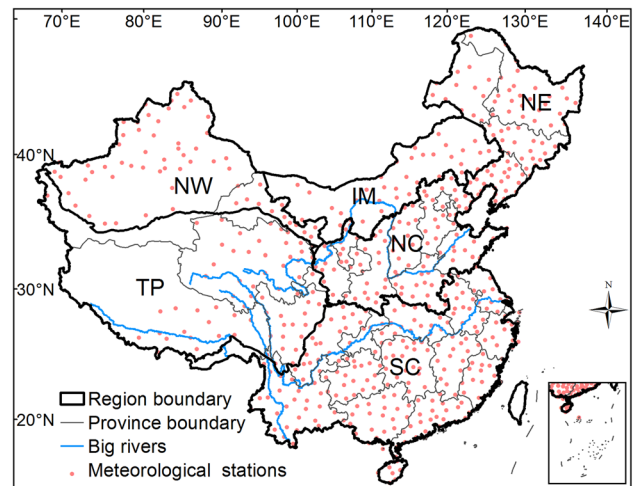
Fig. 1 Distribution of the 581 meteorological stations and the six geographical regions of China, namely Northeast China (NE), Inner Mongolia (IM), Northwest China (NW), Northern China (NC), Southern China (SC) and Tibetan Plateau (TP)

Meteorological Administration (CMA) and were downloaded from the CMA website (http://cdc.cma.gov.cn/index.jsp). Observation stations were deleted from the dataset if (1) the station was opened after 1961, (2) the location of the station changed during the study period, (3) the station was removed before 2010 or (4) more than 5% of the data from the station were missing. For stations with less than 5% of their data missing, the observed values at the same station in other years (before and after the missing year) were averaged to fill gaps in the data. The gap-filling method is based on the assumption that data are missing completely at random. To meet the model input requirements, ground-based point meteorological data were interpolated on a 10×10 km grid using a thin plate spline method.

For the purposes of this study and to provide a better illustration of regional differences, China is divided into six regions, which are as follows: Northeast China (NE), Inner Mongolia (IM), Northwest China (NW), Northern China (NC), Southern China (SC) and the Tibetan Plateau (TP) (Fig. 1).

2.2 Reference evapotranspiration

In general, ET_o reflects the maximum water demand needed to maintain the water balance in the environment, while P reflects the water supply over large areas. Since it is difficult to obtain observed data for ET_o over large areas, ET_o is generally simulated through the use of models. In this study, ET_o was simulated with the modified Penman–Monteith model recommended by the Food and Agricultural Organization, hereafter referred to as the FAO56–PM model (Allen et al. 1998), which can provide precise simulations of both arid

and humid environments. Radiation in the model is calculated by an Ångström formula and its accuracy is determined by empirical coefficients that have regional limitations. In our previous studies, solar radiation for China was calibrated in the FAO56–PM model. As the model was able to effectively represent the AHCR in China (Yin et al. 2008), it was used to calculate the monthly ET_o in this study:

$$ET_o = \frac{0.408\Delta(R_n - G) + \gamma \frac{900}{T+273} U_2(e_s - e_a)}{\Delta + \gamma(1 + 0.34U_2)} \tag{1}$$

where Δ is the slope of the saturated vapor pressure curve (kPa °C^{-1}), R_n is the net radiation (MJ m^{-2} day^{-1}), G is the soil heat flux density (MJ m^{-2} day^{-1}) considered as null for daily estimates, T is the monthly mean air temperature (°C) at 2 m calculated as the average of the maximum and minimum temperatures, U_2 is the average wind speed at a height of 2 m (m s^{-1}), e_s is the saturation vapor pressure (kPa), e_a is the actual vapor pressure (kPa), (e_s–e_a) is the saturation vapor pressure deficit (*VPD*, kPa) at temperature T and γ is the psychrometric constant (0.0677 kPa °C^{-1}).

R_n in the model is calculated by an empirical formula and its accuracy is determined by empirical coefficients that have regional limitations. This study used the following equations to estimate R_n (Yin et al. 2008):

$$R_n = R_{ns} - R_{nl} \tag{2}$$

$$R_{ns} = (1 - 0.23)\left(0.198 + 0.787\frac{n}{N}\right)R_{so} \tag{3}$$

$$R_{nl} = \sigma\left[\frac{T_{max,k}^4 + T_{min,k}^4}{2}\right](0.56 - 0.25\sqrt{e_a})\left(0.1 + 0.9\frac{n}{N}\right) \tag{4}$$

where R_{ns} is the net shortwave radiation (MJ m^{-2} day^{-1}), R_{nl} is the net longwave radiation (MJ m^{-2} day^{-1}), σ is the Stefan–Boltzmann constant (4.903×10^{-9} MJ K^{-4} m^{-2} day^{-1}), $T_{max,k}$ is the maximum temperature (K), $T_{min,k}$ is the minimum temperature (K), R_{so} is the extraterrestrial radiation (MJ m^{-2} day^{-1}), n is the actual sunshine hours and N is the potential sunshine hours. N and R_{so} are calculated by the equations recommended by Allen et al. (1998). Compared with observations from 30 validation stations across China, the calibrated solar radiation was proven to have a relatively

high degree of accuracy (correlation coefficient = 0.952, root mean-square error = 1.729 MJ m^{-2} day^{-1}, mean bias error = 0.030 MJ m^{-2} day^{-1}) (Yin et al. 2008).

2.3 Classification of the AHCR

Following Budyko (1974), the aridity index (*AI*) combines first-order climatic drivers and is calculated as the ratio of annual ET_o and *P*. The index is an indicator of regional humid or arid conditions and is, therefore, a suitable criterion for classifying the AHCR. According to Wu et al. (2005), the *AI* is conventionally used to classify large-scale land surfaces into four zones. These are humid, sub-humid, semi-arid and arid, and are represented by specific natural potential vegetation types, namely forest, forest steppe (including meadow), steppe and desert, as shown in Table 1.

2.4 Impact assessment of ET_o and *P*

Detrending of time series is one of the quantitative ways of effectively assessing the influence of climatic variables on ET_o and *AI* (Huo et al. 2013; Li et al. 2017; Liu et al. 2010; Xu et al. 2006). This study has removed the linear trends from ET_o and *P* so that their contributions to the *AI* can be quantitatively evaluated, which helps to further understand the impact of atmospheric water balance on shifts in the AHCR. The *AI* was then recalculated and compared with the original *AI*. The ratio of the difference between the original and recalculated *AI* was deemed as the change in the *AI* caused by the trend in ET_o or *P*.

As in Eq. (5), based on the least-squares fit of a straight line to the original series $x(t)$ (t = 1961, 1962, 1963,…, 2010), this study computed and subtracted the predicted series $y(t)$, added the first prediction value $y(1961)$ and generated the detrended series $x_{detrend}(t)$. When the trend was removed, the time series was then stationary. As the starting points were the same, this study was also able to compare the detrended and the original data. As in Eqs. (6) and (7), *AI* was recalculated using the detrended ET_o and original *P*, or the original ET_o and detrended *P*, and then compared with its original series. Finally, the percentage ratio of the difference in the *AI* was calculated.

$$x_{detrend}(t) = x(t) - y(t) + y(1961) \tag{5}$$

$$Ratio_{ETo}(t) = \frac{AI(t) - \frac{ETo_{Detrend}(t)}{P(t)}}{AI(t)} \times 100\% \tag{6}$$

Table 1 Criteria for demarcating AHCR of China according to the aridity index (Wu et al. 2005)

AHCR	Aridity index ($AI = ET_o/P$)	Typical natural potential vegetation
Humid region	AI < 1.0	Forest
Sub-humid region	1.0 ≤ AI < 1.5	Forest steppe (including meadow)
Semi-arid region	1.5 ≤ AI < 4.0	Steppe, meadow steppe, and desert steppe
Arid region	AI ≥ 4.0	Desert

$$Ratio_P(t) = \frac{AI(t) - \frac{ETo(t)}{P_{Detrend}(t)}}{AI(t)} \times 100\% \qquad (7)$$

3 Results

### 3.1 Changes in the aridity index

There was considerable spatial variation in the linear trends of the annual *AI* over the past 50 years from 1961 to 2010, as illustrated in Fig. 2a. The annual values of the *AI* showed linear decreasing trends at approximately 62.82% of the stations, mainly in NW, TP, the southern part of NE, and the region south of the Huai River. The trend was tested in the *AI* time series over the last five decades across China with the Mann–Kendal method and it was found that there were statistically significant decreasing and increasing trends at 11.02 and 3.61% of stations, respectively. The significant negative trends were mostly in NW and in the north of the TP, while the significant positive trends were mainly in the west of NC. The spatial distribution of the coefficients of variation (CV) in the annual *AI* across China is displayed in Fig. 2b. More than 60% of the CV values, mainly at stations in NE, SC, and across most of the TP, were between 0.1 and 0.3. Almost 30% of the stations, mainly in the east of NC, most parts of IM, and in the north of NW, had CV values between 0.3 and 0.5. Approximately 5.34% of the stations, mainly in the south of NW, had CV values greater than 0.5. This analysis shows that there was relatively large inter-annual variability in the annual *AI* in NC, IM, and, in particular, in NW.

The frequency distribution of trends in climatic factors across different regions in China is shown in Fig. 3. The *AI* decreased at most stations in NW and SC because of decreases in ET_o and increases in *P*. While ET_o increased at most stations in TP, *P* increased at a larger proportion of stations, which resulted in a decrease in *AI*. The *AI* most likely decreased across IM because the decreasing trend in ET_o was stronger than the decreasing trend in *P*. The increase in the *AI* in NC reflects the fact that, while *P* and ET_o both decreased, *P* decreased at a greater number of stations than ET_o.

3.2 Spatial and temporal changes in AHCR

The area of the semi-arid region in China increased significantly at an average annual rate of 0.116% ($p < 0.001$) over the period from 1961 to 2010 (Fig. 4f). While the area of both the humid and sub-humid regions increased slightly, the area of the arid region declined significantly at a rate of -0.129% per year ($p < 0.001$). The percentages of the area of AHCR in China over recent decades were obtained by calculating the decadal averages of the annual *AI* (Table 2). The result of the statistical t test showed that the area of semi-arid region in the 1990s and the 2000s was significantly different ($p < 0.05$) to the area in the 1960s, as was the area of the arid region. By the 2000s, the semi-arid region had expanded by about 33.53%, and the arid region had decreased by 20.75%, relative to the areas they had covered in the 1960s, which suggests that the semi-arid region in China have expanded as the arid region have contracted over the past five decades.

The spatial distribution of inter-decadal changes in the AHCR in China over the last 50 years is shown in Fig. 4a–e. The percentages of the area of AHCR in certain
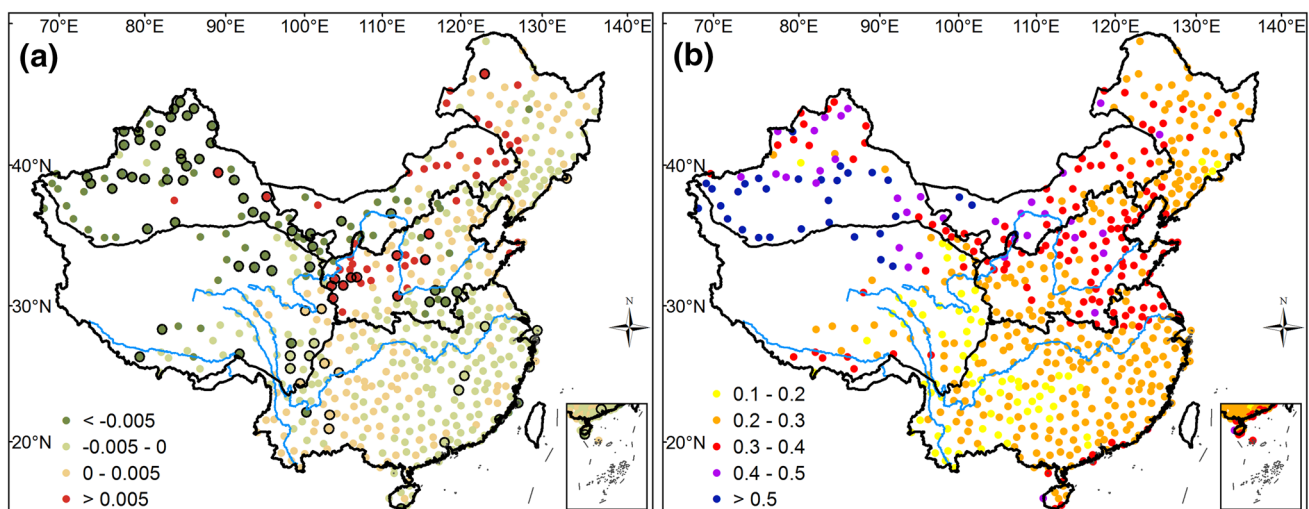

Fig. 2 Spatial distribution of **a** linear trends and **b** CVs in the annual *AI* across China from 1961 to 2010. Circles with an outline in **a** denote statistical significance ($p < 0.05$)
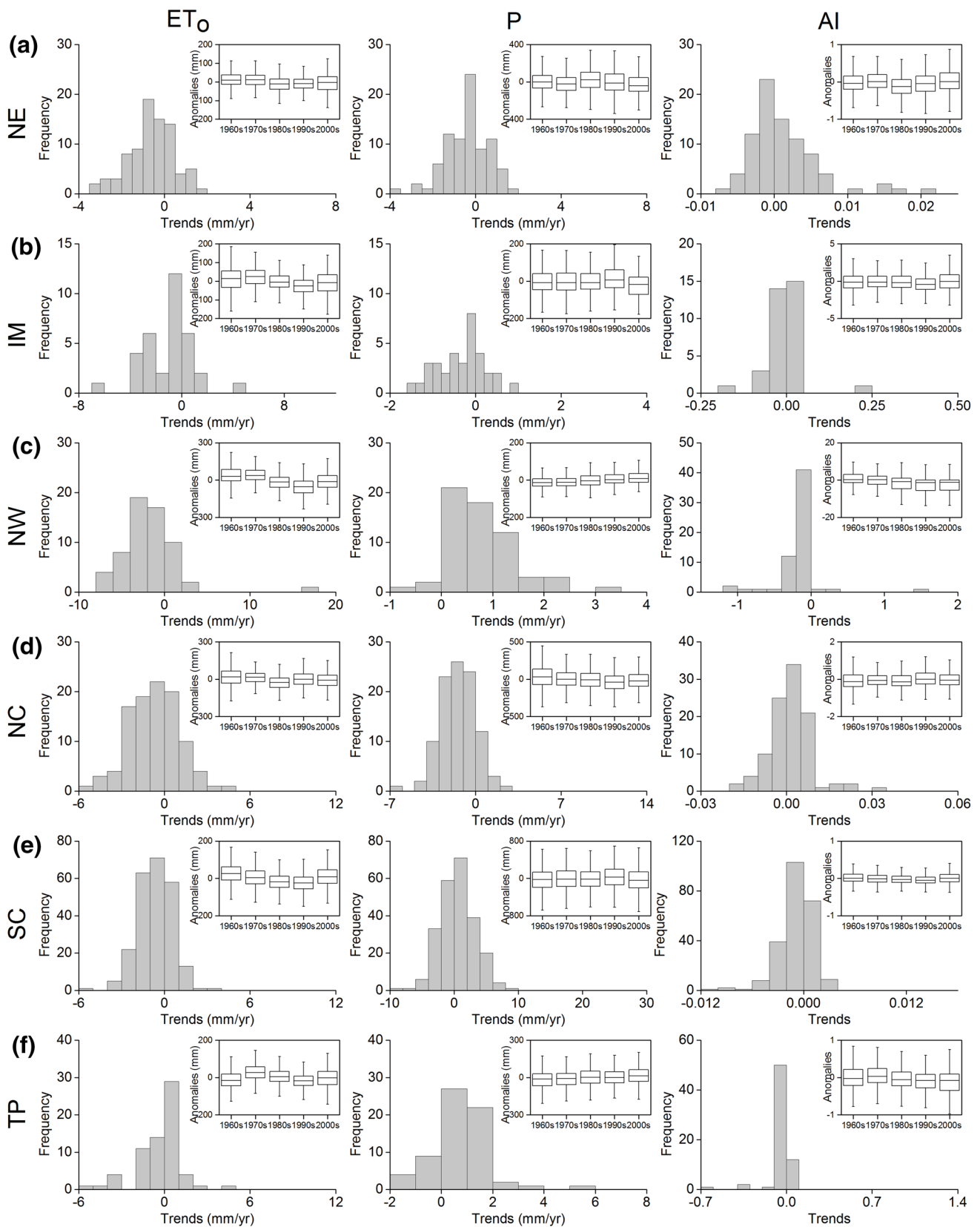
Fig. 3 Frequency distribution of changes in the *AI, ET*o, and *P* across different geographical regions in China from 1961 to 2010. The inset panels show the boxplots of anomalies from 1961 to 2010. The box shows the 25th–75th percentile range, while the median value is shown as a solid line within each box, and outliers are represented by whiskers
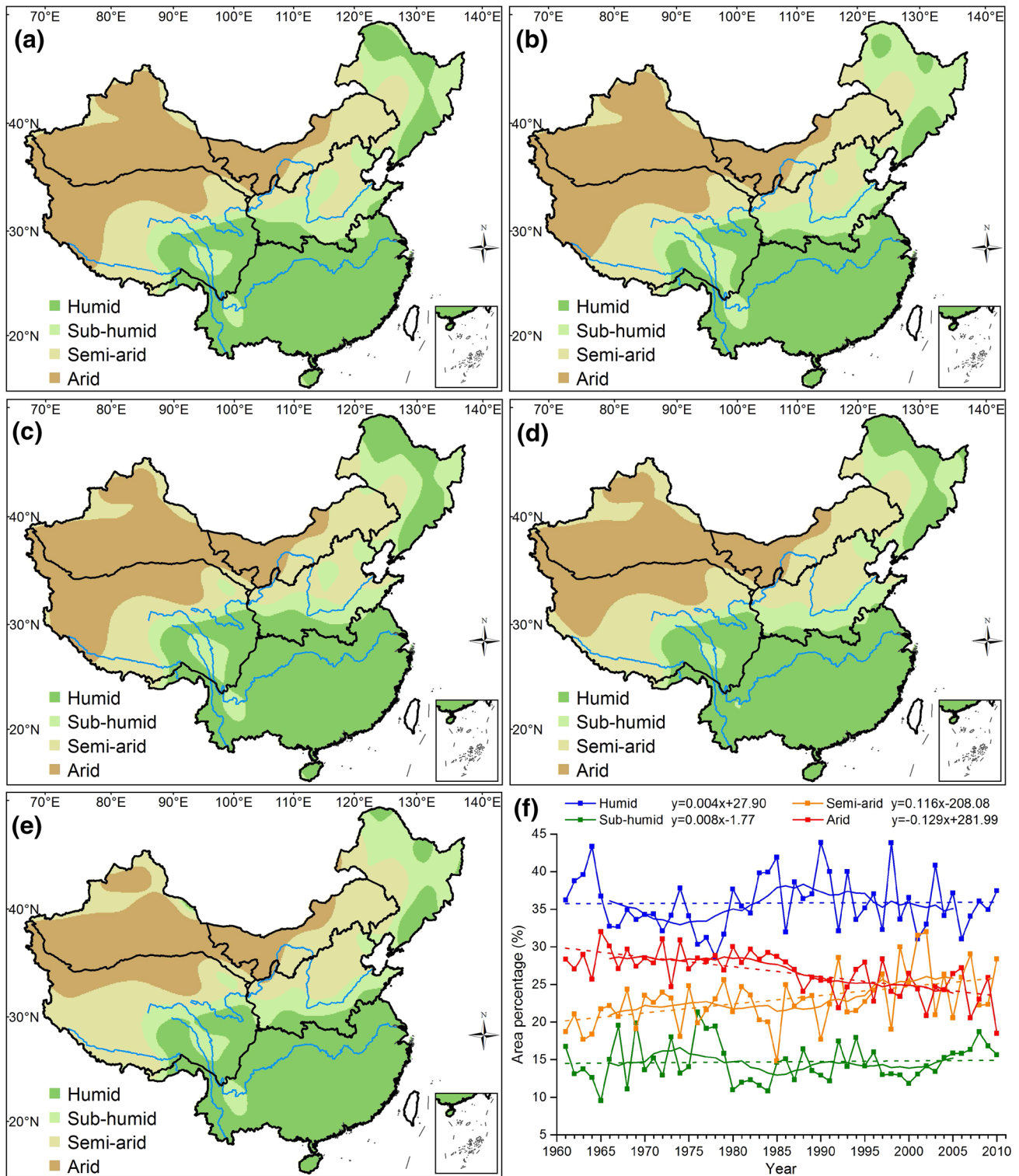
Fig. 4 Spatial distribution of inter-decadal changes in the AHCR across China from **a** 1961 to 1970, **b** 1971 to 1980, **c** 1981 to 1990, **d** 1991 to 2000, **e** 2001 to 2010, and **f** the area percentage (%) from 1961 to 2010. Solid lines with no symbol give the 11-year running means of the data. Dashed lines are the linear fits

Table 2 Inter-decadal percentage (%) changes in the area of AHCR in China from the 1960s to 2000s and changes (%) relative to the 1960s

	Humid		Sub-humid		Semi-arid		Arid	
	Area	Area changed	Area	Area changed	Area	Area changed	Area	Area changed
1960s	34.97		14.71		20.64		29.68	
1970s	31.59	− 9.67*	17.06	15.98	21.76	5.43	29.59	− 0.30
1980s	36.80	5.23	13.39	− 8.97	20.99	1.70	28.82	− 2.90
1990s	36.35	3.95	12.22	− 16.93	25.38	22.97*	26.05	− 12.23*
2000s	33.78	− 3.40	15.15	2.99	27.56	33.53*	23.52	− 20.75*

The asterisk denotes statistical significance ($p < 0.05$) with the t test

geographical regions are as follows. It can be seen that the semi-arid region increased most in TP, NW and NC between the 1960s and the 2000s. Meanwhile, evident decreases were found in the arid region of TP and NW, the sub-humid region of NC and the humid region of NE.

In NW, the area of the semi-arid region grew continuously from 10.96% of NW in the 1960s to 21.80% of NW in the 2000s, and the area of the arid region shrank from 88.79 to 76.98% over the same period (Fig. 4a–e). The shifts in the AHCR were mainly confined to the northern section, as shown by the statistically significant negative trends in the annual *AI*. Correspondingly, the decadal anomalies in the *AI* and in ET_o and *P*, the factors that controlled it, meant that the semi-arid region in NW grew continuously. Specifically, the *AI* was negative from the 1980s, mainly because of increases in precipitation and decreases in ET_o (Fig. 3c). However, while there were significant decreasing trends in the annual *AI*, the original characteristics of most of the NW area did not fundamentally change as it was still mainly characterized by arid conditions with vulnerable ecotopes.

In general, there were obvious changes in the spatial patterns of the AHCR in NE on the inter-decadal time scale (Fig. 4a–e). The humid region occupied 34.77% of NE in the 1960s, but, by the 1970s, it had shrunk considerably to about 19.19%, while, at the same time, the sub-humid region had expanded from 44.46 to 58.98%. In the 1980s and 1990s, the humid region expanded even further to 46.56 and 41.90%, respectively, and the spatial patterns in the AHCR were quite similar. In the 2000s, the humid region shrank again to 20.69% of NE and covered an area that was similar to what it had occupied in the 1970s. The semi-arid region changed only slightly before the 1990s but it grew strongly thereafter, from 18.33% in the 1990s to 25.07% in the 2000s.

In NC, the sub-humid region has decreased noticeably while the semi-arid region has increased over the past five decades. The humid area also grew and replaced the sub-humid area in the 1980s. The area of the humid region decreased from 20.82% of NC in the 1980s to 8.82% of NC in the 1990s, while the sub-humid and semi-arid regions increased by 3.16% and 8.88%, respectively. It is worth mentioning that a separate patch that was previously sub-humid became semi-arid. By the 2000s, the area of the sub-humid region had decreased to 34.98% of NC, its smallest extent.

In TP, the areas of the humid and sub-humid regions changed only slightly from the 1960s to the 2000s, whereas the area of the semi-arid region grew substantially with considerable corresponding reductions in the arid region. Of the different climatic regions, the arid region accounted for the highest percentage of the total area of TP over the first three decades. However, it shrank considerably from almost 41% to about 34% of TP in the 1990s, which was similar to the area occupied by the semi-arid region. Before the 2000s, the arid region was mainly confined to the northern section and part of the western section, but its area decreased by 9.77% from the 1990s to the 2000s, with most loss occurring in the west. However, the semi-arid region increased by 6.72% and extended towards the west of TP. Comparison of the 1960s with the 2000s shows that the areas of the semi-arid and arid regions changed by 13.24% and 16.45%, respectively.

The spatial distribution of shifts between different AHCRs in China for 1971–1980, 1981–1990, 1991–2000 and 2001–2010 relative to 1961–1970 is shown in Fig. 5. A shift was deemed to have occurred in a grid cell if its AHCR type in the 1970s, 1980s, 1990s, or 2000s was inconsistent
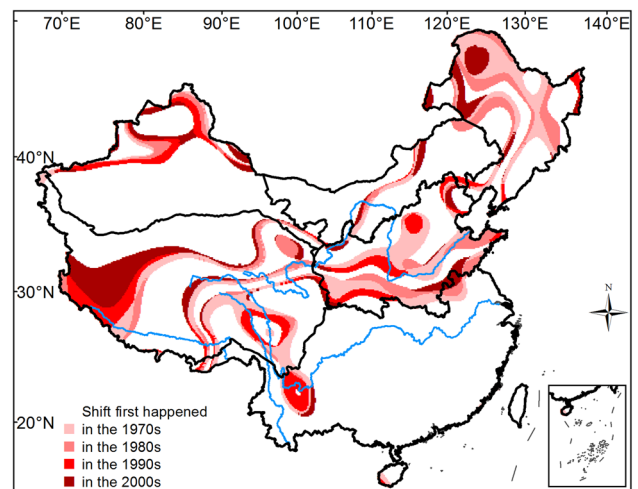

Fig. 5 Spatial distribution of the first shifts in the AHCR across China from the 1970s–2000s relative to the 1960s

with its AHCR type in the 1960s. Generally, 24.14% of the area in China underwent at least one shift, mostly in the northern parts of the country. Based on this study's classification of geographical regions, the NE experienced most changes, with shifts across 47.96% of the region, followed by the NC, where 47.80% of the area changed. There were shifts across 31.8% of TP, mainly in the central and western parts, while there were shifts across 14.66% of NW, mainly the northern part. Relatively small areas of IM and SC, accounting for 8.88 and 6.26%, respectively, experienced shifts. Shifts that first occurred in the 1970s, 1980s, 1990s, and 2000s relative to the 1960s accounted for 8.33, 5.27, 4.84, and 5.69% of the total area of China, respectively. However, when the spatial patterns in the AHCR across China over the past five decades are examined (Fig. 4a–e), it can be seen that there were complicated changes in the humid and sub-humid regions, with boundaries shifting back and forth, while obviously the semi-arid region saw the most expansion.

3.3 Enlargement of the semi-arid region

In order to confirm and explicate the enlargement of the semi-arid region in China, the abrupt annual change in the area of AHCR from 1961 to 2010 was tested by using the Mann–Kendall method, which detected a change point in the semi-arid region around 1985/1986 ($p < 0.05$). Moreover, the statistical t test also showed a significant difference in the annual mean area of the semi-arid region between both before and after 1985/1986 (Table 3). For 1986–2010, the semi-arid region was calculated to have increased by 25.13% relative to the 20.81% of China that it had covered in 1961–1985. Meanwhile, the area of the sub-humid region and arid region decreased by 10.02 and 16.05%, respectively.

Based on this time division, the shifts between different AHCRs in China were analysed over the two 25-year periods. Figure 6 shows all the shifts in the semi-arid regions, namely the shifts between semi-arid and other AHCR types. On the one hand, the area of newly formed semi-arid regions that had been arid regions and sub-humid regions occupied 4.82 and 1.34% of China, respectively. On the other hand, the semi-arid region that had transitioned to arid and sub-humid regions accounted for 0.05 and 0.88% of the area of China, respectively. Thus, the net area change in the semi-arid region was 5.23% of China. The expansion
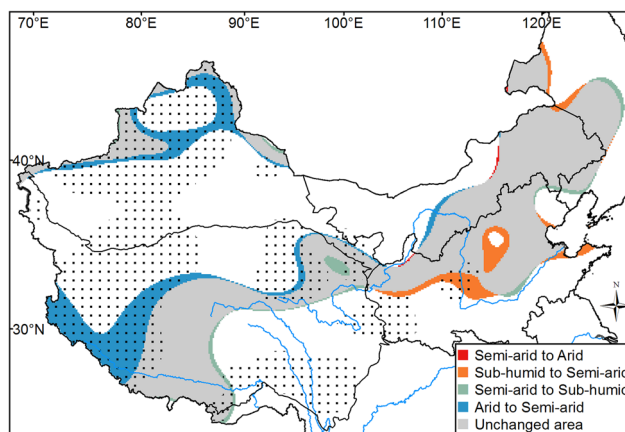
Fig. 6 Spatial distribution of changed and unchanged semi-arid regions in China for 1986–2010 relative to 1961–1985. The stippled area denotes statistical significance ($p < 0.05$) with t test in the annual *AI* between the two periods

of the semi-arid region mainly happened in TP, NW and NC, where it accounted for 11.14, 10.70 and 9.71% of their respective areas. In NC, growth of the semi-arid region was mainly south of the Loess Plateau to the sub-humid region. The semi-arid region in the western TP grew northwards towards the arid region, while the semi-arid region in the northern NW expanded along the basin to the arid region. Generally, the semi-arid region expanded due to shifts from arid regions in the western parts of China (i.e., IM, NW, and TP) and from sub-humid regions in the eastern parts of China (i.e., NE and NC).

In addition to this, the statistical t test was also performed at each grid to examine whether the means of the annual *AI* between the two 25-year periods were different at the 5% significance level (Fig. 6). Results showed that *AI* had significantly changed in about 76.3% of the area of expanded semi-arid regions. This might imply that the enlargement of the semi-arid region in China from 1961–1985 to 1986–2010 was most significant.

3.4 The role of ET_o and *P* in the expansion of the semi-arid region

To further quantify how climatic factors contributed to the enlargement of the semi-arid region, the contributions of ET_o and *P* to *AI* were measured after removing their trends

Table 3 Percentage (%) changes in the area of AHCR in China from 1961–1985 to 1986–2010 and changes (%) relative to 1961–1985

	Humid		Sub-humid		Semi-arid		Arid	
	Area	Area changed	Area	Area changed	Area	Area changed	Area	Area changed
1961–1985	33.94		15.47		20.81		29.79	
1986–2010	35.02	3.18	13.92	− 10.02	26.04	25.13*	25.01	− 16.05*

The asterisk denotes statistical significance ($p < 0.05$) with the t test

(Fig. 7). ET_o mainly decreased over the expanded semi-arid region in NW over the past 50 years, with most grids having values between -4 and -1 mm/year. P, in turn, showed an increasing trend and ranged from 1 to 2 mm/year. The contrasting trends in ET_o and P had consistent effects on the direction of the trend in AI. There was a slight difference between the original and the recalculated AI with detrended ET_o (P) early in the study period, with a change ratio of -1.25% (-3.50%) in the 1960s. As time went by, it became greater and reached -13.39% (-38.05%) in the 2000s. On
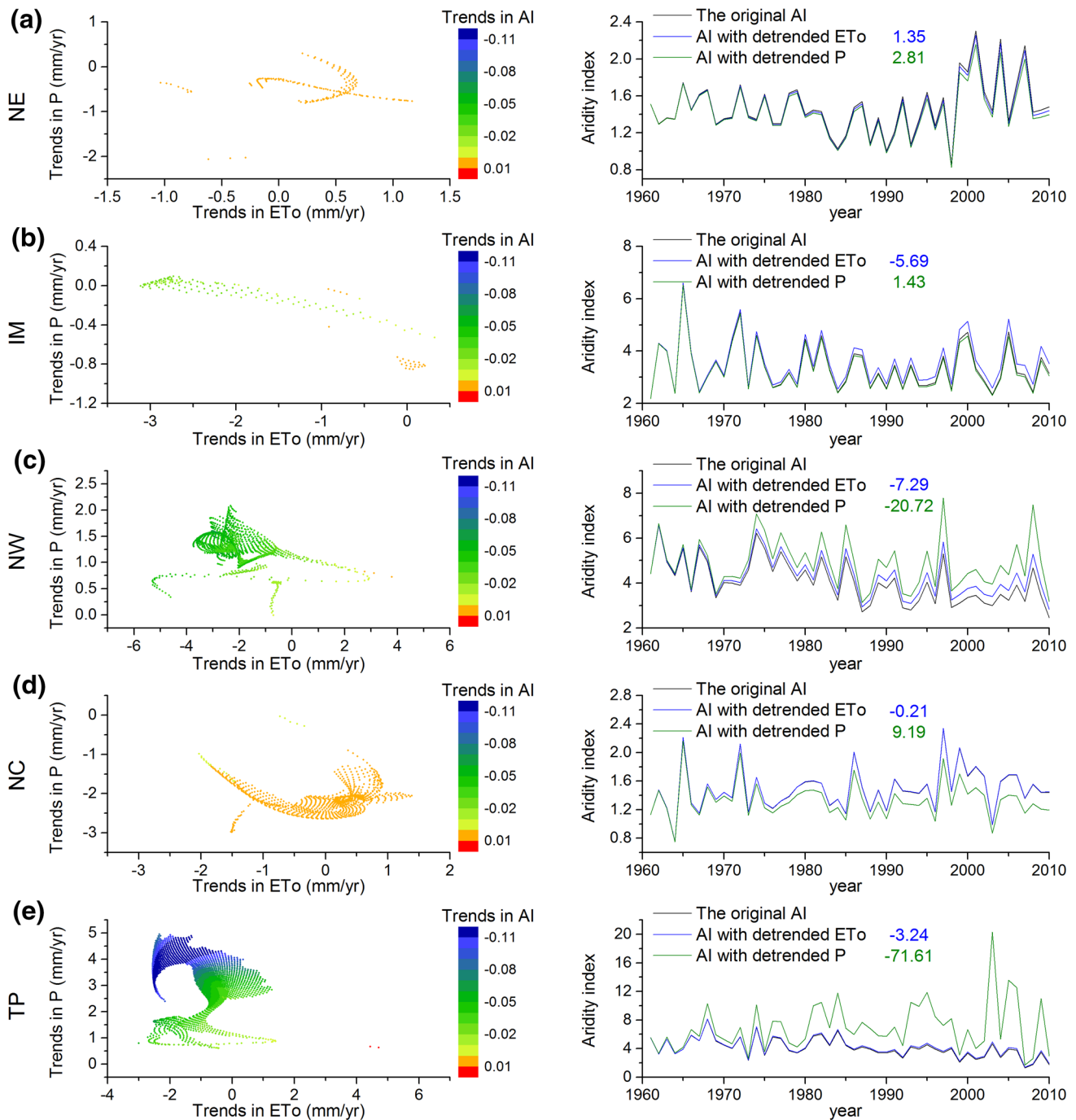
Fig. 7 Linear trends in the AI, ET_o, and P (left column) and comparison between the original AI and the AI recalculated with the detrended ET_o or P (right column) in the expanded area of the semi-arid region across different geographical regions in China from 1961 to 2010. The blue numbers in the right column indicate the change ratios of AI with the detrended ET_o, and the green numbers indicate the change ratios of AI with the detrended P

average, *AI* decreased by ratios of -7.29 and -20.72%, because of the decrease in ET_o (-2.11 mm/year, $p < 0.05$) and the increase in *P* (1.27 mm/year, $p < 0.05$), respectively (Fig. 7c).

The expanded area of the semi-arid region in TP and NW experienced similar changes. The trends in ET_o and *P* were mainly between -2 and 1, and 1 and 5 mm/year, respectively. The difference of the original *AI* from the recalculated *AI* gradually amplified during the past five decades. From the 1960s to the 2000s, the change ratio of *AI* with detrended ET_o ranged from -0.59 to -6.06%, while that with detrended *P* ranged from -10.64 to -140.91%. Due to the decrease in ET_o (-1.02 mm/year) and the increase in *P* (3.02 mm/year, $p < 0.05$), the *AI* decreased by average ratios of -3.24 and -71.61%, respectively (Fig. 7e). This shows that the transition from arid to semi-arid in NW and TP reflected the combined influence of the decreasing trend in ET_o and the increasing trend in *P*. In contrast, the tendency for *P* to increase was an important factor in the expansion of the semi-arid region.

ET_o and *P* showed declining trends in most grids in the expanded area of the semi-arid region in IM and NC. Trends in ET_o ranged from -3 to 0 mm/year and from -2 to 1 mm/year in IM and NC, while those in *P* ranged from -0.5 to 0 mm/year and from -3 to 0 mm/year, respectively. Correspondingly, the *AI* decreased in most grids in the expanded area of the semi-arid region in IM and increased in most grids in the corresponding area in NC. Generally, the significant decrease in ET_o (-1.88 mm/year, $p < 0.05$) caused the *AI* to decline by an average of -5.69% in the expanded area of the semi-arid region in IM (Fig. 7b), and the significant decrease in *P* (-2.13 mm/year, $p < 0.05$) resulted in an average increase of 9.19% in the *AI* for the expanded area of the semi-arid region in NC (Fig. 7d). In the expanded area of the semi-arid land in NE, the combined influence of the increase in ET_o and the decrease in *P*, while not significant, caused the *AI* to increase slightly (Fig. 7a).

4 Discussion

This study has assessed changes in the AHCR from the balance between the water demand and supply and found that the semi-arid region expanded over the period from 1961 to 2010. The semi-arid zone, which is mainly at the boundary of the monsoon belt in China, is susceptible to environmental change (Yang et al. 2005). The enlargement of the semi-arid region illustrated in this study is consistent with the results of earlier studies (Li and Ma 2013; Zhang and Yan 2014). In their analysis of combined soil moisture levels in the twentieth century, Li and Ma (2013) found that the semi-arid and semi-humid climate zones were expanding southeastwards, especially in northern China. From cluster

analysis using K-means of monthly temperature and precipitation for the period from 1966 to 2005, Zhang and Yan (2014) found that the boundary between an arid temperate zone and a sub-humid temperate zone in China was moving eastward. The results of this study generally agree with those of Huang et al. (2016b), who, from their analysis of the ratio of annual precipitation to annual reference transpiration, recently reported global expansion of semi-arid regions over the period from 1948 to 2008. This study also found that the semi-arid region had enlarged mainly because of transfers from arid regions in western China, including NW, TP, and IM, and from sub-humid regions in eastern China, including NC and NE. Due to limitations with regard to the sparse distribution of meteorological stations in TP, there is relatively high uncertainty associated with the AHCR changes in TP.

There has been a relatively good understanding of changes in the individual climatic factors that are related to moisture conditions. Many studies have reported significant decreasing trends in ET_o over a range of scales, from regional to continental, over the last half-century (Dolman and de Jeu 2010; Hobbins et al. 2004; Kukal and Irmak 2016; Peterson et al. 1995; Roderick and Farquhar 2002; Schimel et al. 1997; Yin et al. 2010). From their synthesis of global studies and discussion of trends in measured pan evaporation estimated from reference evapotranspiration, McVicar et al. (2012) reported widespread decreases in the evaporative demand, while Wu et al. (2016) identified distinctive regional patterns in annual total precipitation, with increases in western China and decreases in eastern China over the period from 1960 to 2012. More specifically, almost all the intensity binned precipitation amounts and frequencies increased significantly in northwest China, and the precipitation amount and frequency mostly decreased in northern and southwestern China over the period from 1960 to 2013 (Ma et al. 2015). However, synthetic effects and their relative contributions to changes in aridity and the corresponding AHCR remain less well understood, with considerable spatial heterogeneity in both uncertainty and temporal fluctuations over recent decades.

There has been considerable spatial and temporal variability in trends in aridity over the last few decades. Recently, observed trends in global dryness have been contradictory and very uncertain (Dai 2013; Feng and Fu 2013; Greve et al. 2014; Mueller and Zhang 2016; Sheffield et al. 2012; Trenberth et al. 2014). Regional increases in aridity have been reported in southwestern Spain for the period from 1951 to 2010 (Moral et al. 2016), and for Iran from 1966 to 2005 (Tabari and Aghajanloo 2013). In contrast, increases in wetness in the eastern US from 1895 to 1990 have been attributed to statistically significant increases in precipitation minus reference evaporation (McCabe and Wolock 2002). Consistent with this study's results, wetness has increased

significantly in the northwest of China (Huo et al. 2013), 91.7% of which has been attributed to the increases in precipitation observed from 1960 to 2010 (Liu et al. 2013). The decreasing trend in reference evapotranspiration, together with the significant increasing trend in precipitation, contributed to the change in aridity in NW and the expansion of the semi-arid region. As well as the combined effects of changes in atmospheric water supply and evaporative demand, there have been corrective effects in some other regions such as NC and IM. For example, the expansion of the semi-arid region in NC reflects how the decrease in the evaporative demand was offset by the decrease in precipitation, while the expansion of the semi-arid region in IM demonstrates that the decrease in evaporative demand outpaced the decreases in precipitation.

Semi-arid regions have unique ecosystems and water conditions (Austin and Vivanco 2006; Morgan et al. 2011; Rotenberg and Yakir 2010; Wei et al. 2007). Shifts in the extent of semi-arid regions have great implications for and may have significant impacts on, water resource use, natural vegetation patterns, land degradation and the global carbon cycle. Generally, an eastward shift in the semi-arid zone in Inner Mongolia would exacerbate the development of desertification. The *AI* has mainly increased in northern China. If the current trend towards decreased humidity continues, it may not be possible to meet the demand for agricultural water meaning that agricultural production may be curtailed in this major grain-producing region. It is thought that semi-arid ecosystems, whose carbon balance is strongly associated with circulation-driven variations in both temperature and precipitation, make a significant contribution to variability in carbon uptake on the global scale (Ahlström et al. 2015; Poulter et al. 2014; Zhang et al. 2016). Enlargement of semi-arid regions would mean an increased contribution to variability in global carbon uptake. Analysis of global trends in aridity shows that severe and widespread droughts are likely to occur in many areas over the next 30–90 years (Dai 2013). Therefore, further analyses of the future shift of AHCR and the relationship with aridity trends and underlying mechanisms would be required in order to mitigate the adverse response of ecosystems to climate change.

5 Conclusions

This study has quantitatively assessed the temporal and spatial changes in AHCR in China using data for atmospheric water demand and supply collected at 581 meteorological stations over the last five decades. It has identified the contributions of changes in the atmospheric water demand and supply to shifts in the region.

There have been inter-decadal variations in the spatial distribution of AHCR across China over the last 50 years. Of the four climatic types, there were significant trends in the arid and semi-arid regions. The semi-arid region increased significantly with a linear upward trend of 0.116%/year (p < 0.001) over the period from 1961 to 2010; in the 1960s, this region accounted for 20.64% of the area of China, but it had increased by 33.53% relative to the area covered in the 1960s by the 2000s. There was a linear decreasing trend of −0.129%/year (p < 0.001) in the arid region, which shrank by 20.75% relative to the 29.68% of China it covered in the 1960s. The newly expanded semi-arid areas were mainly in TP, NW and NC, while the arid areas mainly decreased in TP and NW.

Changes in precipitation and evaporative demand have either collaborative or counteractive effects on the extension of the semi-arid region. The decreased reference evapotranspiration together with significant increases in precipitation contributed to the expanded semi-arid region in western China, whereas the significantly decreased precipitation accompanied by decreases in evaporative demand led to the expanded semi-arid region in eastern China. For the enlargement of the semi-arid region in NW, TP and NC, the trend in precipitation was the dominant factor.

Compliance with ethical standards

References

Ahlström A et al (2015) The dominant role of semi-arid ecosystems in the trend and variability of the land CO_2 sink. Science 348:895–899. https://doi.org/10.1126/science.aaa1668

Allen RG, Pereira LS, Raes D, Smith M (1998) Crop evapotranspiration - guidelines for computing crop water requirements. FAO Irrigation and drainage paper 56. United Nations Food and Agriculture Organization, Rome

Austin AT, Vivanco L (2006) Plant litter decomposition in a semi-arid ecosystem controlled by photodegradation. Nature 442:555–558. https://doi.org/10.1038/nature05038

Bailey RG (2009) Ecosystem geography: from ecoregions to sites, 2nd edn. Springer, New York

Budyko MI (1974) Climate and life. Academic Press, New York

Chan D, Wu QG, Jiang GX, Dai XL (2016) Projected shifts in Köppen climate zones over China and their temporal evolution in CMIP5 multi-model simulations. Adv Atmos Sci 33:283–293. https://doi.org/10.1007/s00376-015-5077-8

Cook BI, Smerdon JE, Seager R, Coats S (2014) Global warming and 21st century drying. Clim Dyn 43:2607–2627. https://doi.org/10.1007/s00382-014-2075-y

Crosbie RS, Pollock DW, Mpelasoka FS, Barron OV, Charles SP, Donn MJ (2012) Changes in Köppen–Geiger climate types under a future climate for Australia: hydrological implications. Hydrol Earth Syst Sci 16:3341–3349. https://doi.org/10.5194/hess-16-3341-2012

Dai A (2011) Drought under global warming: a review. WIREs clim change 2:45–65. https://doi.org/10.1002/wcc.81

Dai AG (2013) Increasing drought under global warming in observations and models. Nat Clim Change 3:52–58. https://doi.org/10.1038/nclimate1633

Dai A, Fung IY, del Genio AD (1997) Surface observed global land precipitation variations during 1900–88. J Clim 10:2943–2962

Dolman AJ, de Jeu RAM (2010) Evaporation in focus. Nat Geosci 3:296. https://doi.org/10.1038/ngeo849

Engelbrecht CJ, Engelbrecht FA (2016) Shifts in Köppen-Geiger climate zones over southern Africa in relation to key global temperature goals. Theor Appl Climatol 123:247–261. https://doi.org/10.1007/s00704-014-1354-1

Feng S, Fu Q (2013) Expansion of global drylands under a warming climate. Atmos Chem Phys 13:10081–10094. https://doi.org/10.5194/acp-13-10081-2013

Feng S, Ho C-H, Hu Q, Oglesby RJ, Jeong S-J, Kim B-M (2012) Evaluating observed and projected future climate changes for the Arctic using the Köppen-Trewartha climate classification. Clim Dyn 38:1359–1373. https://doi.org/10.1007/s00382-011-1020-6

Fraedrich K, Gerstengarbe FW, Werner PC (2001) Climate shifts during the last century. Clim Change 50:405–417. https://doi.org/10.1023/a:1010699428863

Fu B, Liu G, Chen L, Ma K, Li J (2001) Scheme of ecological regionalization in China. Acta Ecol Sin 21:1–6 **(Chinese)**

Gerstengarbe FW, Werner PC (2009) A short update on Koeppen climate shifts in Europe between 1901 and 2003. Clim Change 92:99–107. https://doi.org/10.1007/s10584-008-9430-0

Greve P, Seneviratne SI (2015) Assessment of future changes in water availability and aridity. Geophys Res Lett 42:5493–5499. https://doi.org/10.1002/2015gl064127

Greve P, Orlowsky B, Mueller B, Sheffield J, Reichstein M, Seneviratne SI (2014) Global assessment of trends in wetting and drying over land. Nat Geosci 7:716–721. https://doi.org/10.1038/ngeo2247

Hobbins MT, Ramirez JA, Brown TC (2004) Trends in pan evaporation and actual evapotranspiration across the conterminous US: paradoxical or complementary? Geophys Res Lett 31:L13503. https://doi.org/10.1029/2004GL019846

Holdridge LR (1967) Life zone ecology. Tropical Science Center, San Jose

Huang B (1989) Outline of the comprehensive physical geographical regionalization of China. Collect Works Geogr 21:10–20 **(Chinese)**

Huang J, Yu H, Guan X, Wang G, Guo R (2016a) Accelerated dryland expansion under climate change. Nat Clim Change 6:166–171. https://doi.org/10.1038/nclimate2837

Huang JP, Ji MX, Xie YK, Wang SS, He YL, Ran JJ (2016b) Global semi-arid climate change over last 60 years. Clim Dyn 46:1131–1150. https://doi.org/10.1007/s00382-015-2636-8

Huo Z, Dai X, Feng S, Kang S, Huang G (2013) Effect of climate change on reference evapotranspiration and aridity index in arid region of China. J Hydrol 492:24–34. https://doi.org/10.1016/j.jhydrol.2013.04.011

IPCC (2013) Summary for policymakers. Working Group I Contribution to the IPCC Fifth Assessment Report Climate Change 2013: The Physical Science Basis. Cambridge University Press, Cambridge

Köppen W (1931) Grundriss der Klimakunde. Walter de Gruyter, Berlin

Kukal M, Irmak S (2016) Long-term patterns of air temperatures, daily temperature range, precipitation, grass-reference evapotranspiration and aridity index in the USA Great Plains: Part I. Spatial trends. J Hydrol 542:953–977. https://doi.org/10.1016/j.jhydrol.2016.06.006

Li MX, Ma ZG (2013) Soil moisture-based study of the variability of dry-wet climate and climate zones in China. Chin Sci Bull 58:531–544. https://doi.org/10.1007/s11434-012-5428-0

Li Y, Yao N, Chau HW (2017) Influences of removing linear and nonlinear trends from climatic variables on temporal variations of annual reference crop evapotranspiration in Xinjiang, China. Sci Total Environ 592:680–692. https://doi.org/10.1016/j.scitotenv.2017.02.196

Lin C (1954) Outline of the physical geographical regionalization. Acta Geogr Sin 20:395–418

Liu Q, Yang ZF, Cui BS, Tao S (2010) The temporal trends of reference evapotranspiration and its sensitivity to key meteorological variables in the Yellow River Basin, China. Hydrol Process 24:2171–2181. https://doi.org/10.1002/hyp.7649

Liu X, Zhang D, Luo Y, Liu C (2013) Spatial and temporal changes in aridity index in northwest China: 1960 to 2010. Theor Appl Climatol 112:307–316. https://doi.org/10.1007/s00704-012-0734-7

Ma S, Zhou T, Dai A, Han Z (2015) Observed changes in the distributions of daily precipitation frequency and amount over China from 1960 to 2013. J Clim 28:6960–6978. https://doi.org/10.1175/jcli-d-15-0011.1

Mahlstein I, Daniel JS, Solomon S (2013) Pace of shifts in climate regions increases with global temperature. Nat Clim Change 3:739–743. https://doi.org/10.1038/nclimate1876

McCabe GJ, Wolock DM (2002) Trends and temperature sensitivity of moisture conditions in the conterminous United States. Clim Res 20:19–29. https://doi.org/10.3354/cr020019

McVicar TR et al (2012) Global review and synthesis of trends in observed terrestrial near-surface wind speeds: implications for evaporation. J Hydrol 416:182–205. https://doi.org/10.1016/j.jhydrol.2011.10.024

Mihailovic DT, Lalic B, Dreskovic N, Mimic G, Djurdjevic V, Jancic M (2015) Climate change effects on crop yields in Serbia and related shifts of Köppen climate zones under the SRES-A1B and SRES-A2. Int J Climatol 35:3320–3334. https://doi.org/10.1002/joc.4209

Moral FJ, Paniagua LL, Rebollo FJ, García-Martín A (2016) Spatial analysis of the annual and seasonal aridity trends in Extremadura, southwestern Spain. Theor Appl Climatol:1–16 https://doi.org/10.1007/s00704-016-1939-y

Morgan JA et al (2011) C_4 grasses prosper as carbon dioxide eliminates desiccation in warmed semi-arid grassland. Nature 476:202–205. https://doi.org/10.1038/nature10274

Mueller B, Zhang XB (2016) Causes of drying trends in northern hemispheric land areas in reconstructed soil moisture data. Clim Change 134:255–267. https://doi.org/10.1007/s10584-015-1499-7

Peterson TC, Golubev VS, Groisman PY (1995) Evaporation losing its strength. Nature 377:687–688

Poulter B et al (2014) Contribution of semi-arid ecosystems to interannual variability of the global carbon cycle. Nature 509:600–603. https://doi.org/10.1038/nature13376

Ren M, Yang R (1961) Physical geographical regionalization in China. Acta Geogr Sin 27:66–74. https://doi.org/10.11821/xb196100005 (Chinese)

Reynolds JF et al (2007) Global desertification: building a science for dryland development. Science 316:847–851. https://doi.org/10.1126/science.1131634

Roderick ML, Farquhar GD (2002) The cause of decreased pan evaporation over the past 50 years. Science 298:1410–1411. https://doi.org/10.1126/science.1075390

Rohli RV, Joyner TA, Reynolds SJ, Shaw C, Vázquez JR (2015) Globally extended Köppen–Geiger climate classification and temporal

shifts in terrestrial climatic types. Phys Geogr 36:142–157. https://doi.org/10.1080/02723646.2015.1016382

Rotenberg E, Yakir D (2010) Contribution of semi-arid forests to the climate system. Science 327:451–454. https://doi.org/10.1126/science.1179998

Rubel F, Kottek M (2010) Observed and projected climate shifts 1901–2100 depicted by world maps of the Köppen–Geiger climate classification. Meteorol Z 19:135–141. https://doi.org/10.1127/0941-2948/2010/0430

Scanlon BR, Keese KE, Flint AL, Flint LE, Gaye CB, Edmunds WM, Simmers I (2006) Global synthesis of groundwater recharge in semiarid and arid regions. Hydrol Process 20:3335–3370. https://doi.org/10.1002/hyp.6335

Schimel DS, Braswell BH, Parton WJ (1997) Equilibration of the terrestrial water, nitrogen, and carbon cycles. Proc Natl Acad Sci USA 94:8280–8283. https://doi.org/10.1073/pnas.94.16.8280

Sheffield J, Wood EF, Roderick ML (2012) Little change in global drought over the past 60 years. Nature 491:435–438. https://doi.org/10.1038/nature11575

Tabari H, Aghajanloo MB (2013) Temporal pattern of aridity index in Iran with considering precipitation and evapotranspiration trends. Int J Climatol 33:396–409. https://doi.org/10.1002/joc.3432

Thornthwaite CW (1948) An approach toward a rational classification of climate. Geogr Rev 38:55–94. https://doi.org/10.2307/210739

Trenberth KE, Dai AG, van der Schrier G, Jones PD, Barichivich J, Briffa KR, Sheffield J (2014) Global warming and changes in drought. Nat Clim Change 4:17–22. https://doi.org/10.1038/nclimate2067

Wei W, Chen LD, Fu BJ, Huang ZL, Wu DP, Gui LD (2007) The effect of land uses and rainfall regimes on runoff and soil erosion in the semi-arid loess hilly area, China. J Hydrol 335:247–258. https://doi.org/10.1016/j.jhydrol.2006.11.016

Wu S, Yin Y, Zheng D, Yang Q (2005) Aridity/humidity status of land surface in China during the last three decades. Sci China Ser D: Earth Sci 48:1510–1518. https://doi.org/10.1360/04yd0009

Wu SH, Zheng D, Yin YH, Lin ED, Xu YL (2010) Northward-shift of temperature zones in China's eco-geographical study under future climate scenario. J Geogr Sci 20:643–651. https://doi.org/10.1007/s11442-010-0801-x

Wu Y, Wu S-Y, Wen J, Xu M, Tan J (2016) Changing characteristics of precipitation in China during 1960–2012. Int J Climatol 36:1387–1402. https://doi.org/10.1002/joc.4432

Xu CY, Gong L, Jiang T, Chen D, Singh VP (2006) Analysis of spatial distribution and temporal trend of reference evapotranspiration and pan evaporation in Changjiang (Yangtze River) catchment. J Hydrol 327:81–93. https://doi.org/10.1016/j.jhydrol.2005.11.029

Yang JP, Ding YJ, Chen RS, Liu LY (2005) Fluctuations of the semi-arid zone in China, and consequences for society. Clim Change 72:171–188. https://doi.org/10.1007/s10584-005-6858-3

Yin YH, Wu SH, Zheng D, Yang QY (2008) Radiation calibration of FAO56 Penman–Monteith model to estimate reference crop evapotranspiration in China. Agric Water Manage 95:77–84. https://doi.org/10.1016/j.agwat.2007.09.002

Yin YH, Wu SH, Chen G, Dai EF (2010) Attribution analyses of potential evapotranspiration changes in China since the 1960s. Theor Appl Climatol 101:19–28. https://doi.org/10.1007/s00704-009-0197-7

Zhang XL, Yan XD (2014) Temporal change of climate zones in China in the context of climate warming. Theor Appl Climatol 115:167–175. https://doi.org/10.1007/s00704-013-0887-z

Zhang Q, Xu CY, Chen X (2011) Reference evapotranspiration changes in China: natural processes or human influences? Theor Appl Climatol 103:479–488. https://doi.org/10.1007/s00704-010-0315-6

Zhang Y et al (2016) Precipitation and carbon-water coupling jointly control the interannual variability of global land gross primary production. Sci Rep 6:39748. https://doi.org/10.1038/srep39748

Zheng D (1999) A study on the eco-geographic regional system of China. FAO FRA2000 Global Ecological Zoning Workshop, Cambridge

Zhu K (1930) Climatic provinces of China. Geogr J 3 **(in Chinese)**